RETINAL IMAGE SEGMENTATION BASED ON DEEP LEARNING

In partial fulfillment of the requirements of

Undergraduate Graduation Thesis

南京信息工程大学

Submitted by

MD JABIR AL HUJAIFA

201953052001

Session 2019

Under the guidance of

Prof. Hai Huan

Department of Electronics and information Engineering

Nanjing University of Information Science and Technology

MAY 2023

Table of Contents

DECLARATION

i. I, Md Jabir Al Hujaifa, solemnly declare that this scientific research work was completed in the spirit of rigor and innovation.

ii. Excluding cited material, all other test, data, and related materials presented in this thesis are true and valid.

iii. This thesis contains the research works and achieved research results that were written personally under the supervision of my supervisor, Prof **HAI HUAN**, and is not to be used for illegal purposes.

iv. Excluding the references and acknowledgement, there haven't been any instances of plagiarism of neither other people's nor another organization's published or written scientific achievements.

v. I further declare that all colleagues who have made contributions to the research conducted in this thesis have been declared and have received acknowledgement.

vi. I acknowledge that any violation of these declarations may result in disciplinary action by the academic institution.

vii. I also acknowledge that the results of this research may be subject to future verification and scrutiny.

viii. I certify that I have read and understood all the regulations and guidelines pertaining to academic conduct and research ethics as set forth by my academic institution.

ix. I accept full responsibility for any errors or omissions contained within the thesis and absolve my academic institution, my supervisor, and any other parties involved from any liability arising from the publication or use of this thesis.

x. Finally, I affirm that this thesis represents my own original work, and that I have not received any unauthorized assistance in its preparation.

(Author Signature)

Date: 2023-04-30

Retinal Image Segmentation Based on Deep Learning

HUJAIFA MD JABIR AL
School of Electronics and information Engineering, NUIST, Nanjing 210044, China

ABSTRACT

One of our most vital senses, eyesight is also one of the most vulnerable to harm from accidents or illnesses like glaucoma and diabetic retinopathy, which can impair vision. While accidents cannot be predicted, breakthroughs in imaging technology allow us to foresee the beginning of illnesses in their early stages. Fast diagnoses may be made using computer vision and image processing skills. In order to help in diagnosis, this study suggests an algorithm that can divide retinal pictures into groups that are healthy or unhealthy, especially diabetic retinopathy and glaucoma. The program looks at which picture transformation is under its purview and which region of the retina aids in precise diagnosis.

The experiment created to aid in the development of the algorithm simultaneously receives all values from a dataset and executes domain transformations one after the other. The scientific history of retinal blood vessel segmentation is thoroughly examined and introduced in this thesis. The reason for segmenting retinal blood vessels, applications already in use, databases that are accessible to the general public, various image segmentation techniques, and current retinal color picture segmentation implementations are only a few of the topics covered in the thesis. The study finds that when employing a bag of visual words and an image category classifier model, the computer program may use blood vessels from fundus pictures after frequency transformation to produce the maximum accuracy for the method. This system properly categorizes retinal pictures into healthy or unhealthy categories, which can help in the early diagnosis of disorders including diabetic retinopathy and glaucoma. The results of the study are crucial because they offer a rapid and painless approach for identifying eye conditions, which can assist medical professionals in initiating therapy early and preventing vision loss. Early illness detection by the algorithm can increase the likelihood of effective therapy and result in patients having a higher quality of life.

The study's findings demonstrate how modern imaging techniques and computer algorithms may greatly enhance the detection and management of eye conditions including glaucoma and diabetic retinopathy. Ophthalmologists and other medical practitioners can benefit from the method since it can accurately predict illness connections by using blood vessels from fundus pictures after frequency transformation.

Key Words: Retinal imaging, Image Processing, Diabetic retinopathy, deep learning, Retinal Blood Vessel Segmentation.

基于深度学习的视网膜图像分割

王宇杰
南京信息工程大学，江苏 南京 210044

摘要

本文我们的视力是最重要的感官之一，但也是最容易受到损伤的，如糖尿病视网膜病变和青光眼等疾病，这些疾病会导致视力丧失。虽然我们无法预测事故，但通过成像技术的进步，我们可以预测疾病在早期阶段的发生。借助计算机视觉和图像处理能力，可以提供近乎即时的诊断。本研究提出了一种算法，可以将视网膜图像分类为健康或不健康的类别，特别是针对糖尿病视网膜病变和青光眼，以帮助诊断。该算法探究了在其范围内哪种图像转换最可行，以及视网膜的哪个部分有助于准确诊断。

为了开发算法，实验同时接受数据集的所有值，并独立地执行域转换。本论文全面调查和介绍了视网膜血管分割的研究背景，包括视网膜血管分割的动机、现有应用程序、公开可用的数据库、几种图像分割算法以及视网膜彩色图像分割的现有实现。该研究得出结论，计算机程序可以在使用视觉词袋和图像类别分类器模型时，利用频率转换后的眼底图像中的血管，为算法提供最高的准确性。该算法可以通过准确将视网膜图像分类为健康或不健康的类别，帮助早期检测糖尿病视网膜病变和青光眼等疾病。该研究的发现具有重要意义，因为它们提供了一种非侵入性和快速的诊断眼科疾病的方法，这可以帮助医生早期开始治疗，避免视力丧失。该算法在早期发现疾病的能力可以提高成功治疗的机会，并为患者提供更好的生活质量。

总之，该研究表明，先进的成像技术和计算机算法可以显著改善糖尿病视网膜病变和青光眼等眼科疾病的诊断和治疗。该算法能够利用频率转换后的眼底图像中的血管，提供高度准确的疾病预测方法，使其成为眼科医生和其他医疗专业人员的宝贵工具。

关键字：视网膜成像、图像处理、糖尿病视网膜病变、深度学习、视网膜血管分割。

Chapter 1

INTRODUCTION

There is a very significant risk of vision loss and blindness from eye conditions such diabetic retinopathy, glaucoma, and age-related macular degeneration, which are growing more and more prevalent. To lower the risk of blindness and visual loss, these illnesses must be diagnosed as early as possible. Technology developments have resulted in the creation of several techniques for acquiring color medical photographs of various body areas, including the retina. The retina, a crucial component of the human eye, serves as a warning sign for eye conditions.

Since fundus images are highly sensitive to vascular diseases, they are essential for screening the human eye. The diagnosis of these disorders may usually be made from the fundus picture. Through the use of image segmentation techniques, retinal blood vessels can be separated from fundus images. Automatic disease diagnosis can be aided by segmenting the retina's picture such that vessel part and non-vessel part are isolated from one another. Images of the retina give critical diagnostic data that aid in identifying whether the retina is healthy or sick.

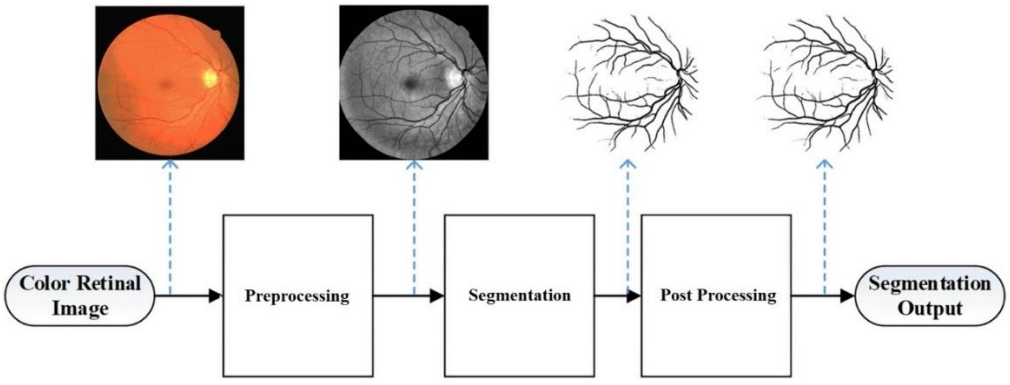

Figure. *Different stages of segmentation*

In the medical community, these pictures are frequently utilized to diagnose vascular and non-vascular disease. Images of the retina can reveal alterations in the retinal vascular network, which are frequently seen in conditions including diabetes, glaucoma, hypertension, cardiovascular disease, and stroke. The reflectivity, tortuosity, and patterns of blood vessels in the retina can alter as a result of several illnesses. For instance, diabetic retinopathy can result in neovascularization, or the growth of new blood vessels, and hypertension can alter the branching angle or tortuosity of vessels. These medical conditions have

the potential to result in vision loss or even blindness if untreated. Early awareness of these changes is essential for taking precautions and avoiding serious vision loss. An effective technique for medical diagnostics is the automatic segmentation of retinal blood vessels from retinal pictures. To separate an object of interest from the background in a picture, segmentation techniques should be as precise and dependable as feasible.

This thesis' main goal is to provide a precise technique of retinal vascular segmentation that can help with illness diagnosis that is done automatically. The thesis will examine numerous picture segmentation methodologies and suggest a brand-new, highly accurate, and reliable way for segmenting retinal vessels. A sizable dataset of retinal pictures will be used to evaluate the proposed method, and its performance will be compared to that of existing techniques. The findings of this research will be extremely helpful in developing precise and dependable techniques for the automated identification of retinal disorders.

1.1 MOTIVATION

WHY RETINAL BLOOD VESSEL SEGMENTATION MATTERS

Segmenting retinal blood vessels manually is a difficult and time-consuming task, and it can be challenging to make a detailed segmentation if the vascular network is complex. Automated segmentation is therefore valuable, as it reduces the time and effort required, and can provide segmentation results as good or better than a manual labelling by an expert. However, for practical applications, it is better to have algorithms that do not depend on configuring many parameters so that non-experts can use this technology with ease. Automated blood vessel segmentation faces challenges related to low contrast in images, a wide range of vessel widths, and the variety of different structures in retinal images such as retinal image boundaries, optic disc, and retinal lesions caused by diseases.

Although different methods are available for retinal segmentation, there is still room for improvement. Most algorithms for retinal blood vessel segmentation focus on automatically detecting diabetic retinopathy, which is now the major cause of blindness. Early detection of diabetic retinopathy can prevent vision loss. Many authors have proposed several different blood vessel segmentation approaches based on different techniques. The complexities and segmentation performances vary among the algorithms. In this thesis, we study and implement different blood vessel segmentation algorithms and compare their performance with the results provided in the literature.

1.2 OBJECTIVES

THE OBJECTIVES OF THIS THESIS:

i. To research and evaluate several image segmentation methods for the segmentation of retinal blood vessels.
ii. To put forth a cutting-edge technique for segmenting retinal vessels that achieves great accuracy and dependability.
iii. Utilizing a sizable dataset of retinal images, compare the performance of the proposed method with that of existing methods.
iv. To determine if the suggested technique may help with the automated detection of different retinal illnesses such glaucoma and diabetic retinopathy.
v. Specifically for glaucoma and diabetic retinopathy, to develop an algorithm that can categorize retinal pictures into healthy or unhealthy categories depending on the existence of blood vessels.
vi. To show the value of the suggested technique in detecting retinal illnesses early, which can assist medical professionals in beginning treatment sooner and preventing vision loss.
vii. viii. To offer insightful information on the creation of precise and trustworthy techniques for the automated detection of retinal illnesses.

1.3 PROBLEM BACKGROUNDS

Globally, glaucoma and diabetic retinopathy are the two leading causes of blindness. While diabetic retinopathy causes a gradual loss of vision as a result of retinal damage brought on by diabetes, glaucoma harms the optic nerve. Early identification is achievable due to the concentration of these disorders in the retina of the human eye and their distinctive beginning symptoms.

While neither disease currently has a permanent cure, early detection can reduce permanent damage and vision loss. Diagnoses may now be established without invasive procedures or blood tests thanks to non-invasive computer imaging technology. The two primary imaging methods for obtaining a retinal picture are fundus photography and optical coherence tomography (OCT).

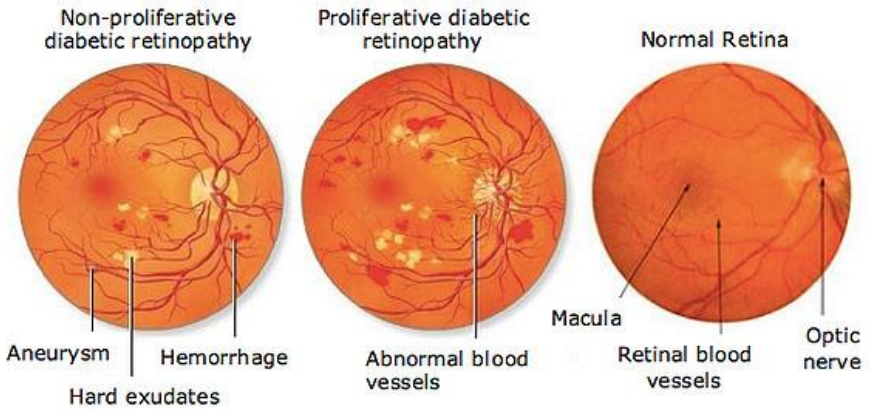

Figure. *Different types of retinal diseases*

Using fundus photography, retinal tissues are depicted in two dimensions by reflecting light onto a plane. The strength of the picture varies with the brightness of the light that is reflected. In contrast, OCT measures the depth of the distance traveled by the light's backward propagation to reveal variations in the refractive indices of different tissue surfaces. The diagnosis and treatment of these illnesses have been made easier by modern imaging methods, which have made it simpler to get a retinal picture.

1.4 RESEARCH QUESTIONS

The two main conditions that cause blindness worldwide are glaucoma and diabetic retinopathy. Early diagnosis is essential for avoiding irreversible harm and visual loss. Fundus photography and optical coherence tomography (OCT), two non-invasive computer imaging techniques, have made diagnosis possible, although there is still potential for improvement in terms of accuracy and reliability.

This thesis' research questions (RQs) attempt to answer the following problem:

i. RQ1: Which fundus imaging characteristics may most accurately describe the retina's state of health in terms of disease association?

ii. RQ2: Which picture transformations, such frequency- or spatial-based transformations, are more effective for diagnosing diseases accurately?

Thesis Outline:

The outline for this thesis is as follows:

- Introduction: Provides context for the issue, problem statements, thesis objectives, and RQs.
- Background: Introduces pertinent areas that are connected to the thesis.
- Related work: Discusses prior research in pertinent disciplines and how it relates to the thesis.
- Method: Describes the experiment's setup, development processes, obstacles encountered, and workarounds for these obstacles.
- Results: Describes the specific outcomes of applying the algorithm to the RQs from section 1.4.
- Analysis and Discussion: Provides specifics on the thesis's assessment techniques.
- Conclusion and Future Work: Presents findings and ideas for more study that may be done to support this theory.

This thesis intends to enhance the diagnosis and management of retinal illnesses by addressing the RQs and offering insights into the creation of precise and trustworthy systems for the automated diagnosis of retinal disorders.

Chapter 2

BACKGROUND STUDY

This chapter provides an explanation of the key terms that are frequently used in the thesis and explains their relevance to the study. Each section introduces the topic and connects it to the overall thesis in two or more paragraphs

2.1 STRUCTURE OF THE HUMAN EYE

Similar to a camera, the human eye is a light-sensitive organ that enables us to view the world around us. The crystalline lens and cornea of the eye serve as a camera's lens, while the iris regulates the quantity of light that reaches the retina by changing the pupil size. The retina, which has light-sensitive photoreceptors, is located in the back of the eye and receives light through the cornea, pupil, and lens. The picture that forms on the retina is converted into electrical impulses and sent via the optic nerves to the brain, where the experience of vision is produced.

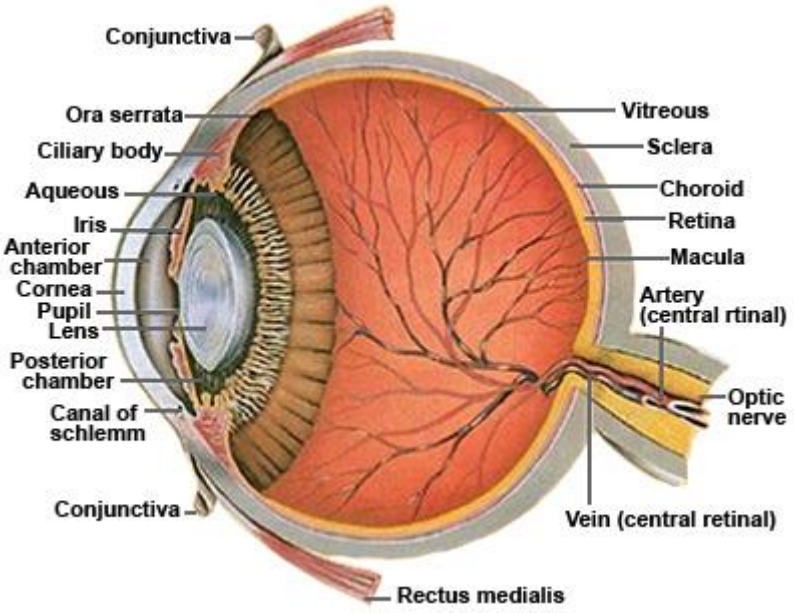

Figure. *Human eye cross section*

Sharp central vision is provided by the macula, a tiny, yellowish region in the center of the retina that has a diameter of around 5.5 mm. It houses the fovea, which is crammed full of cone photoreceptors and is what gives humans their trichromatic color vision. There are no rod photoreceptors that can detect brightness in the fovea. In the visible region of the electromagnetic spectrum, L-, M-, and S-cone cells are sensitive to long, medium, and short wavelength ranges, although rod cells do not detect color.

The visible portion of the optic nerve, where blood vessels and fibers of the optic nerve enter the eye, is known as the optic disc. It is also known as a blind spot since it lacks rod or cone photoreceptors. The optic disc is where the retinal arteries and veins emerge, with arteries normally being thinner than veins. Being able to see at least 20/20 with normal vision makes the macula an essential component of the eye. Figure shows the macula fovea, the optic disc, the veins, and the arteries.

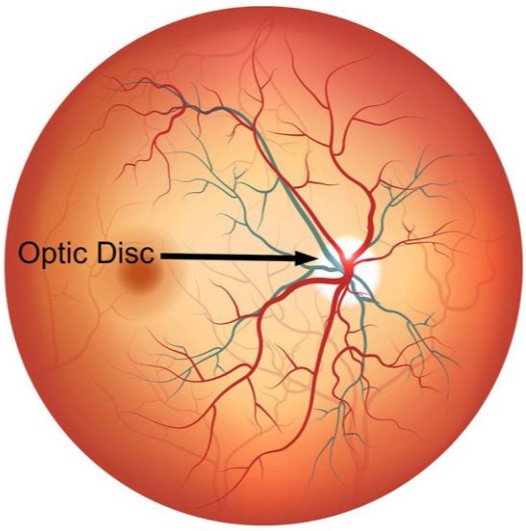

Figure. *Human eye optic disc*

2.2 COMPUTER VISION

The goal of computer vision is to automate routine human operations using visual aids by allowing computers to understand and react to visual media in the real world. Its main objective is to extract dimensional real-world data, analyze that data to create computer-readable judgments or numerical qualities. In the area of processing medical images, computer vision has grown in importance recently. A variety of imaging data sources are available, including x-rays, ultrasounds, fundus pictures, and tomographs.

The volume of data that has to be processed makes human processing challenging and necessitates the use of automated solutions. Numerous such tools have been created, one of which is the computer vision toolkit made available by Mathworks in its MATLAB software. The processing of medical pictures is supported by a variety of features and functions provided by this toolkit. The application of computer vision in medical research and practice is expanding as medical image processing increases in significance.

2.3 IMAGE PROCESSING

This thesis heavily relies on image processing, and the appropriate processes of image enhancement, transformation, and segmentation are essential for correctly evaluating medical pictures. These methods enable the improvement of picture quality and the extraction of pertinent data from the images, which may be applied to subsequent investigations and study. It is a field of science where photographs are analyzed for future research. The following image processing stages are pertinent to this thesis:

1. ***Image enhancement:*** Used to increase the image's quality.
2. ***Picture transformation:*** The use of mathematical procedures to a picture to change its default spatial domain or frequency domain. While the image is processed as pixels in the spatial domain, it is processed as intensity in the frequency domain.
3. ***Image segmentation:*** The process of dividing areas of interest into more manageable chunks.

2.3.1 IMAGE ENHANCEMENT:

The initial stage of image processing, called image enhancement, tries to raise a picture's quality by boosting its sharpness, contrast, detailing, and noise-removal. The main objective of image enhancement is to provide a clean image with distinct objects so that segmentation is simpler.

Two of the many approaches used in picture enhancement are as follows:

1. Histogram equalization: This image processing method redistributes the intensity values of the pixels in a picture to increase contrast. A stronger contrast picture with improved visual quality is produced by mapping the original pixel intensity distribution to a more uniform distribution.

Histogram equalization may be described mathematically as follows:

1. Calculate the histogram of the input picture f(x,y), where the cumulative distribution function (CDF), also known as the cumulative distribution function (CDF), is defined as:

$$CDF(i) = \sum H(j), j=0 \text{ to } i$$

2. The cumulative frequency of all pixels with intensity values less than or equal to i is mapped from the pixel intensity value i by the CDF.
3. To get the histogram equalization transformation function T(i), normalize the CDF as follows:

$$T(i) = (L-1) * CDF(i) / MN$$

Here, L is the total number of pixels in the image, and MN is the number of possible pixel intensity values (typically 256 for an 8-bit image).

4. To produce the histogram-equalized output picture g(x,y), which is defined as:

$$g(x,y) = T(f(x,y))$$

5. apply the transformation function T(i) to each pixel in the input image f(x,y).
   The contrast and aesthetic appeal of the picture are improved because to the more equal distribution of pixel intensity values in the final image.

2. Contrast-Limited Adaptive Histogram Equalization (CLAHE): A form of histogram equalization called Contrast-Limited Adaptive Histogram Equalization (CLAHE) is used to boost an image's contrast without over-emphasizing local features or amplifying noise. The contrast amplification inside each of the smaller sections is constrained to a predetermined maximum value by CLAHE, which splits the picture into smaller parts and conducts histogram equalization on each region independently.

The CLAHE procedure can be described mathematically as follows:

1. Create MxM non-overlapping square sections from the supplied picture f(x,y).
2. To get the equalized picture g(x,y) in each region, compute the histogram of each region and then use histogram equalization.
3. Reduce the pixel values in each area to a predetermined range, such as [0, L-1], where L is the total number of pixel intensity values that may be used (256 for an 8-bit picture, for example).
4. To get the final CLAHE output picture h(x,y), combine the equalized areas.

2.3.2 IMAGE TRANSFORMATION

Mathematical procedures that may change an image from one domain to another are referred to as image transformations. Two significant domain changes that are pertinent to this thesis are:

1. Spatial Domain Filters: A spatial domain filter is a type of image processing technique that works directly with an image's pixel values. These filters are widely used to enhance or modify specific characteristics of a picture, such as edges or textures, by conducting a convolution operation on the image matrix.

A spatial domain filter can be conceptualized mathematically as follows:

$$f(x+i, y+j) * h(i, j) = g(x, y)$$

Here, the input image is represented by f(x+i, y+j), the output image is represented by g(x, y),

and the convolution kernel or filter mask is represented by h(i, j). The kernel is often a tiny matrix with various weight values that is odd in size (e.g., 3x3, 5x5, etc.).

Let's use a straightforward averaging filter with a 3x3 kernel as an illustration:

$$\begin{matrix} 1 & 1 & 1 \\ 1 & 1 & 1 \\ 1 & 1 & 1 \end{matrix}$$

We would slide the kernel over each pixel in the input picture and calculate the weighted average of the pixel values in the kernel window to apply this filter on the image. For instance, the calculation would be as follows if the filter were to be applied to the pixel at position (2,2) in the image:

$$g(2, 2) = (1*f(1, 1) + 1*f(1, 2) + 1*f(1, 3) + 1*f(2, 1) + 1*f(2, 2) + 1*f(2, 3) + 1*f(3, 1) + 1*f(3, 2) + 1*f(3, 3)) / 9$$

To produce the filtered output picture, this technique would be repeated for each pixel in the original image. The averaging filter is employed in this instance to blur the image and lessen noise.

2. Frequency Domain Filters: Frequency domain filters are a form of image processing method that work with an image's frequency elements rather than its pixel values directly. These filters are frequently employed to reduce noise or highlight particular frequency-domain aspects of a picture.

The Fourier transform, which breaks an image down into its component frequencies, may be used to depict an image in the frequency domain. The amplitude and phase of each frequency component are shown by the intricate function known as the Fourier transform of a picture.

A frequency domain filter can be described mathematically as:

$$G(u, v) = H(u, v)F(u, v)$$

The input image's Fourier transform is represented by F(u, v), the filter transfer function is represented by H(u, v), and the output image is represented by G(u, v).

The frequency response of the filter is described mathematically by the transfer function, H(u, v). Depending on the intended outcome, it can be built to boost some frequency components while suppressing others.

The converted output image is subjected to the inverse Fourier transform to produce the filtered output picture in the spatial domain:

$$g(x, y) = F^{-1}\{G(u, v)\}$$

The filtered output picture in this case is g(x, y), and F1 stands for the inverse Fourier transform.

High-pass, low-pass, and band-pass filters are a few types of frequency domain filters. These filters are frequently employed in edge detection, noise reduction, and picture enhancement applications in the field of image processing.

2.3.3 IMAGE SEGMENTATION:

The process of segmenting an image into various areas or segments, each of which represents a different item or component of an object inside the picture, is known as image segmentation. It's a crucial job in computer vision and image processing since it makes it possible to extract useful information from digital images.

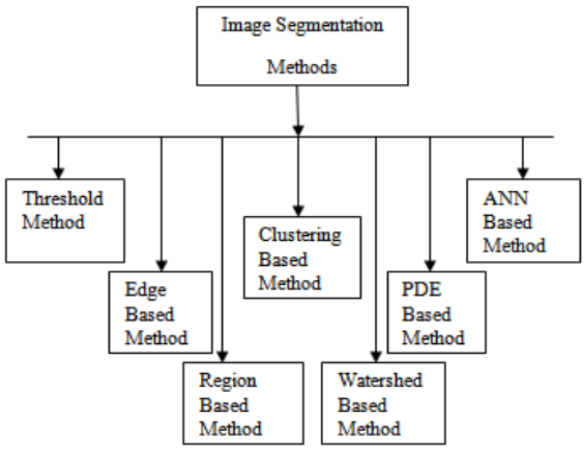

Figure. *There are different types of image segmentation*

1. Edge Detection: Edge detection is a fundamental method of image processing that locates the edges of objects in an image. In order to identify the edges or contours of objects, it detects abrupt differences in intensity levels between neighboring pixels in an image.

In terms of mathematics, edge detection is the technique of locating areas in a picture where there is a noticeable shift in intensity values. The conventional method for accomplishing this is to apply an operator or filter to the picture that enhances the edges while suppressing the other areas. Let Gx and Gy be the horizontal and vertical gradient operators, and let I be the input picture. Mathematically, the Sobel operator is expressed as follows:

$$G = sqrt\ (Gx\text{^}2 + Gy\text{^}2)$$

where G is used to detect the edges in the picture and represents the gradient's strength at each individual pixel. Other edge detection algorithms include the Canny operator, which soothes the image before detecting the edges at various scales, and the Laplacian of Gaussian (LoG) operator, which applies the Laplacian operator after applying a Gaussian filter to the image in order to detect the edges.

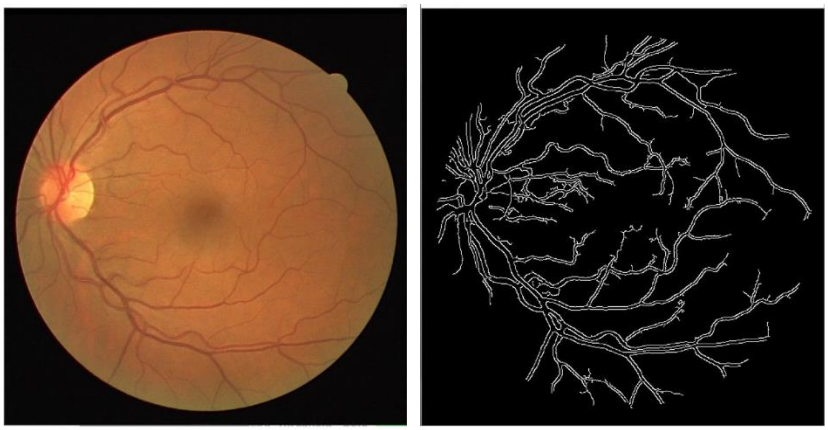

Figure. *Image of input retinal fundus image and its image after edge detection is applied.*

2. Thresholding: Setting a threshold value and categorizing each pixel in the picture as either foreground or background depending on whether its intensity value is above or below the threshold is the straightforward image segmentation technique known as thresholding. This method is frequently applied to photographs with plain backgrounds where the main subjects stand out against it clearly.

Thresholding may be described mathematically as follows:

Let T be a threshold value and I be an input picture with dimensions M x N. The thresholding process can be shown as follows:

$$If\ I(i,j) >= T,\ then\ B(i,j) = 1$$

$$If\ I(i,j) < T,\ then\ B(i,j) = 0$$

where B is the binary output picture of size M x N, where each pixel represents the foreground or background, respectively, by being either 0 or 1. For the thresholding procedure to be successful, the threshold value T must be chosen carefully. It should be properly selected so that it can efficiently distinguish between the foreground and backdrop.

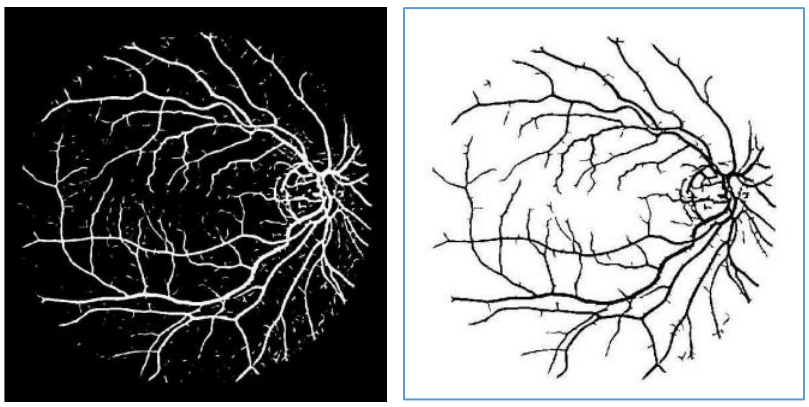

(a) (b)

Figure. *The image after the threshold operation (b) The image after length filtering*

3. Region-based Segmentation: Using a technique called region-based segmentation, pixels are grouped into areas according on how similar their colors, textures, or other properties are. To do this, clustering pixels into areas that minimize a cost function that assesses pixel similarity is necessary.

Region-based segmentation may be defined mathematically as follows:

Assume that I input picture with dimensions M x N and that R is a collection of regions R1, R2..., Rk. Each region Ri is described as a collection of pixels with a common texture or color.

The goal of region-based segmentation is to divide the picture into a number of regions R while minimizing the cost function J.

The cost function J calculates the degree of similarity and degree of dissimilarity between pixels within an area. Depending on the application and the attributes of the picture, the cost function can be defined in a variety of ways. The Mumford-Shah functional is a well-liked cost function used in region-based segmentation and is provided by:

$$J(R) = \sum i=1k\, \lambda| Ri | + \mu\int Ri\, (I(x) - c\_i)^2\, dx + v\sum(i,j)\in E|c\_i - c\_j|^2$$

where, and v are regularization parameters, Ri is the i-th region, | Ri | is the region's size, I(x) is the pixel's intensity value, c_i is the region's mean intensity value, and E is a collection of nearby regions. The cost function's first term penalizes the amount of regions, while the second term gauges how similar pixels inside a region are to one another, and the third term gauges how different pixels are between adjacent regions.

The region-based segmentation may be accomplished after the cost function has been specified by reducing the cost function using optimization techniques like graph-cut or mean-shift clustering.

2.4 ANALYZING THE RESULT:

2.4.1 CONFUSION MATRIX

In machine learning, a confusion matrix is a potent tool for assessing how well a categorization model is doing. It compares the anticipated and actual class labels of a series of data points to offer a thorough assessment of the model's performance. Four primary terms—TP, TN, FP, and FN—represent the true positive, true negative, false positive, and false negative predictions, respectively, in the confusion matrix.

i. **True Positive (TP)** is a measurement of how many occurrences the model accurately identified as positive. This indicates that the model properly distinguished the data point's positive class.

ii. **True Negative (TN)** is the measure of how many occurrences the model properly identified as negative. This indicates that the model properly distinguished the data point's negative class.

iii. **False Positive (FP)** refers to the number of cases where the model predicts erroneously that the class is positive when it is really negative. This indicates that a data point that really belongs to the negative class was predicted by the model to be in the positive class.

iv. **False Negative (FN)** refers to the number of cases when the model predicts a class as negative when it really belongs to a positive one. This signifies that a data point that really belongs to the positive class was predicted by the model to be in the negative class.

v. **Condition Positive (P)** denotes the total amount of instances that fall within the positive category. P, then, is the number of data points overall that truly fall into the positive category.

vi. **Condition negative (N)** The number of occurrences that fall within the negative class is denoted by the condition negative (N). N thus stands for the total amount of data points that genuinely fall into the negative category.

Other performance metrics can be computed based on the values in the confusion matrix in addition to these terms. These measures, which offer a more thorough study of the model's performance, include accuracy, recall, and F1 score.

2.4.2 INFERENCES FROM THE CONFUSION MATRIX

The confusion matrix examines the true positive, true negative, false positive, and false negative predictions of a classification model in order to offer crucial information on the performance of the model. In order to evaluate the model's performance and identify potential improvement areas, it helps to calculate metrics like accuracy, recall, and precision.

i. **Accuracy:** This statistic indicates how frequently the classifier predicts correctly. It is determined by dividing the total number of occurrences by the sum of true positive and true negative values.

$$\text{Accuracy}=TP+TN/\text{total}$$

ii. **Recall:** The genuine positive value is divided by the total number of positive cases to arrive at the recall metric, which indicates how frequently the algorithm accurately predicts positive occurrences.

$$Recall=TP/P$$

iii. **Precision:** This measure, which is determined by dividing the true positive value by the total of true positive and false positive values, reveals the percentage of true positive predictions among all positive predictions generated by the model.

$$Precision=TP/TP+FP.$$

These conclusions provide us a clearer picture of how well a classification model is performing and show us where it might be improved. We may enhance the model's accuracy, precision, and overall efficacy in predicting class labels by making adjustments depending on these criteria.

The confusion matrix can be shown mathematically as follows:

	Actual Positive	**Actual Negative**
Predicted Positive	True Positive (TP)	False Positive (FP)
Predicted Negative	False Negative (FN)	True Negative (TN)

In this instance, the columns correspond to the expected classification (positive or negative), whereas the rows correspond to the actual classification (positive or negative). True positives (TP) are the number of occurrences that were correctly identified as positive, whereas true negatives (TN) are the number of cases that were correctly classed as negative. False negatives (FN) are cases of positive that were mistakenly categorized as negative, whereas false positives (FP) are instances of negative that were mistakenly classed as positive.

Chapter 3

EXISTING RESEARCH AND DATASETS

This section covers the previous studies and research conducted in the area of interest relevant to this thesis. It explains how this prior work has helped identify a problem area that needs to be addressed.

3.1 ADVANCES IN RETINAL IMAGE PROCESSING

3.1.1 A BRIEF HISTORY

With the development of algorithms to compare pictures of healthy and diseased retinas in the 1980s, retinal imaging achieved considerable advancements. The first attempts at processing retinal images date back to 1973, when Matsui et al. segmented blood vessels on angiography slides using morphological methods. By using top-hat filters on angiograms, the first technique to segment anomalies suggestive of diseases was created in 1984. Revolutionary developments in digital image processing throughout the 1990s brought retinal image processing up to date with current research standards.

3.1.2 CONTEMPORARY RESEARCH

A critical stage in the processing of retinal pictures for the recognition and diagnosis of various retinal disorders is retinal image segmentation. Due to its capacity to learn hierarchical features from significant volumes of data, deep learning-based techniques have been increasingly popular in the segmentation of retinal images in recent years.

Ronneberger et al.'s 2015 [1] presentation of a fully convolutional neural network (FCN) for the semantic segmentation of medical pictures was one of the first efforts in this field. Numerous following efforts on medical image segmentation, including those on retinal image segmentation, were influenced by this study.

A deep learning-based technique for retinal vascular segmentation utilizing a fully convolutional network (FCN) with a skip-connection architecture was proposed by Fu et al. in 2016 [2]. On some benchmark datasets, the suggested technique produced results that were state-of-the-art.

A unique adversarial learning-based retinal vascular segmentation algorithm was later suggested by Zhang et al. in 2018 [3]. They discovered the mapping from retinal pictures to binary vessel maps using a generative adversarial network (GAN). When compared to cutting-edge approaches, the suggested method produced better vessel segmentation results.

Other retinal structures have also been segregated using deep learning-based methods in addition to segmenting vessels. As an illustration, Li et al. suggested a deep learning-based technique for segmenting the optic disc in retinal pictures [4]. To precisely segment the optic disc, they utilized a fully convolutional network with a boundary loss function.

Recently, attention-based deep learning methods have been suggested for segmenting retinal images. As an illustration, Qiu et al. suggested a unique attention-based U-Net for segmenting retinal vessels [5]. On some benchmark datasets, the suggested technique produced results that were state-of-the-art..

In conclusion, approaches for segmenting retinal pictures based on deep learning have shown good results. These methods could improve retinal image processing's accuracy and efficacy, which might aid in the early detection and diagnosis of a number of retinal diseases.

3.2 RETINAL BLOOD VESSEL DATABASES

The technique of recognizing and removing blood vessels from retinal pictures is called retinal blood vessel segmentation. The databases of retinal blood vessels are used by researchers to create and test segmentation algorithms. These databases offer retinal color pictures and the associated data, such as vessel ground truth images that show where each vessel pixel is located.

Currently, only four of the nine publicly accessible retinal blood vessel databases provide vessel ground truth pictures. These four databases—CHASE DB1, DRIVE, HRF, and STARE—are frequently used to assess various approaches for segmenting retinal blood vessels. The most utilized databases among these are DRIVE and STARE.

These freely accessible datasets enable academics to create and test their algorithms in a consistent manner, making it simpler to evaluate the effectiveness of various approaches. This has allowed researchers to build on earlier findings and create more precise and effective algorithms for this job, which has resulted in substantial breakthroughs in the area of retinal blood vessel segmentation.

3.2.1 DRIVE DATASET

To facilitate comparative research on the segmentation of blood vessels in retinal pictures, the DRIVE (Digital Retinal pictures for Vessel Extraction) database was created. It comprises of 40 color retinal photos gathered from a Dutch study for detecting diabetic retinopathy. The photographs were taken with a non-mydriatic camera that had a field of view of 45 degrees, and they were compressed using the JPEG format. Each image has been cropped to have a field of view that is circular and has a diameter of around 540 pixels. A mask picture that indicates the field of view is offered for each image.

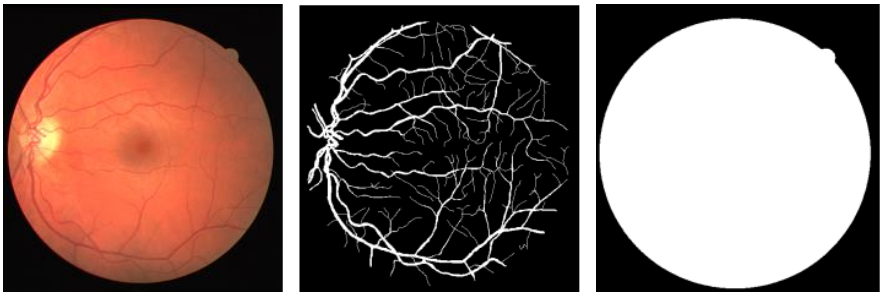

(a) (b) (c)

Figure. *A sample from the DRIVE dataset.* ***(a)*** *The training image;* ***(b)*** *the manual of the training image;* ***(c)*** *the training mask of the image.*

The 40 photos were split into a training set and a test set, each of which had 20 images. In contrast to the test photos, which feature two manual segmentations of the vasculature, the training images only have one. Human observers taught to designate all pixels for which they were at least 70% convinced that they were vessels carried out these manual segmentations. Only 7 abnormal retinal images in the DRIVE database exhibit mild disease, indicating generally good image quality.

Researchers researching retinal blood vessel segmentation can benefit from the DRIVE database since it contains both normal and pathological retinal pictures. The offered manual segmentations can be used as a yardstick to assess how well computer-generated segmentations perform in comparison to those made by human observers.

3.2.2 STARE DATASET

The US National Institutes of Health provided funding for a study started at the University of California, San Diego that includes the STARE (Structured Analysis of the Retina) database. It includes 400 retinal color photos that were taken using a Topcon TRV-50 fundus camera, which had a roughly 650 by 500-pixel field of vision. 20 of the 400 photos feature ground truth images that can be used to segment blood vessels. Two experts manually segmented these 20 photos, and the second expert's segmented findings include far more thin vessels than the results of the first expert.

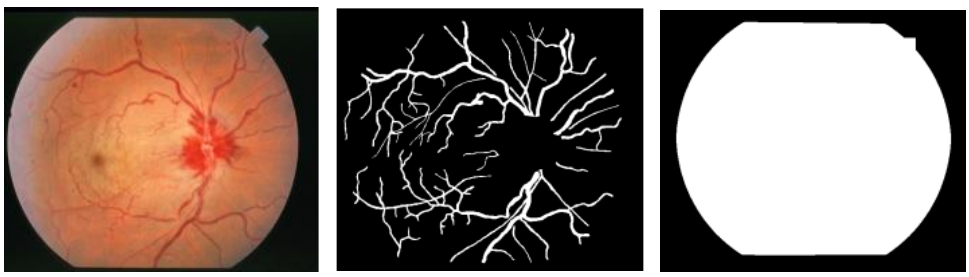

(a) (b) (c)

Figure. *A sample from the Structure Analysis of the Retina (STARE) data set.* ***(a)*** *An image;* ***(b)*** *the first manual segmentation;* ***(c)*** *the second manual segmentation.*

Only nine of these 20 images represent the retina in a healthy state, while the other 11 display symptoms of eight different retinal diseases, some of which are mild and some of which are severe.

Three of the photos also exhibit a loss of clarity. The STARE database, which is the most intricate of all the datasets for retinal blood vessels, is frequently used to assess how well segmentation algorithms withstand noise.

The STARE database is a useful tool for researchers looking at the segmentation of retinal blood vessels despite its complexity. It is possible to compare various segmentation approaches in difficult situations thanks to the availability of both healthy and sick photos with ground truth segmentation.

3.2.3 CHASE DB1

Children of different ethnic backgrounds' retinal scans can be found in the CHASE DB1 database, a portion of the CHASE (Child Heart and Health Study in England) dataset. Only this subset of CHASE has access to vessel ground truth images. The retinal pictures were taken with a Nidek Co. Ltd., Gama Gori, Japan-made handheld NM-200-D fundus camera. The photos are tagged image files (TIF) with a resolution of 1280 by 960 pixels and a 35-degree field of view. The photos were taken in dim lighting with the flash on and the illumination set to 3, and the photographer adjusted the levels to prevent overexposure or underexposure.

There are a total of 28 photos in the CHASE DB1 database, taken from the left and right eyes of 14 kids. Two human observers manually segmented the vessel ground truth photos. Although none of the 28 retinal images have any known symptoms, they are all of good quality and contrast.

Figure. *A sample from the CHASE_DB1 dataset. (**a**) An image; (**b**) the first manual segmentation; (**c**) the second manual segmentation.*

The CHASE DB1 database is a useful tool for researchers looking at retinal blood vessel segmentation, especially for children of several ethnicities because it contains ground truth photographs. Under standardized settings, the high-quality photos with vessel ground truth segmentation may be used to assess and compare the effectiveness of various segmentation techniques.

3.2.4 HRF

A joint research team created the HRF (High-Resolution Fundus) image collection to allow comparative studies on automated segmentation algorithms on retinal fundus pictures. A Canon CR-1 fundus camera with a 45-degree field of view and various acquisition settings was used to take the photos. There are 45 fundus pictures altogether in the HRF segmentation dataset, comprising 15 photos

of healthy patients, 15 images of diabetic retinopathy patients, and 15 images of glaucoma patients. Each image has a set of ground truth images for vascular segmentation that were created by a team of retinal image analysis specialists and doctors from partnering ophthalmology clinics. The HRF database's photos have the best resolution of all retinal blood vessel datasets, measuring 3504 by 2336. The pictures are represented mathematically by matrices of size 3504 by 2336, where each member corresponds to a pixel value.

The HRF database is a useful tool for researchers looking at retinal blood vessel segmentation since it has high-resolution pictures with ground truth segmentation for both healthy and diseased retinas. The dataset may be used to assess and contrast the effectiveness of various segmentation methods under controlled circumstances.

3.3 PERFORMANCE MEASURE

True positive (TP) pixels are those that have been correctly recognized as being from a vessel, whereas true negative (TN) pixels are those that have been correctly identified as being from a non-vessel. Contrary to false positive (FP), which refers to non-vessel pixels that have been classified as vessels, false negative (FN) refers to vessel pixels that have been segmented as non-vessel pixels.

To determine the possibility that the segmentation technique would effectively find vessel pixels, sensitivity is determined as follows:

$$\text{Sensitivity} = \frac{Total\ TP}{Total\ Tp + Total\ FN}$$

Specificity is the probability that non-vessel pixels will be identified by the segmentation approach. When determining specificity:

$$\text{Specificity} = \frac{Total\ TN}{Total\ TN + Total\ FP}$$

Accuracy is a measure of a segmentation method's overall performance and is calculated using:

$$\text{Accuracy} = \frac{Total\ TN + Total\ TP}{Total\ TN + Total\ FP + Total\ Tp + Total\ FN}$$

The area under a receiver operating characteristic (ROC) curve, also known as AUC, which is determined using both sensitivity and specificity, displays the performance of segmentation. In this study, AUC was calculated using the procedure described in [39,40,41]:

$$\text{AUC} = \frac{Sensitivity + Specivity}{2}$$

It highlighted that a segmentation that has an AUC of 0.50 or below is useless and simply dependent on guessing, whereas a segmentation that has an AUC of 1 may precisely segment every pixel.

Chapter 4

IMPLEMENTATION

This chapter aims to provide a clear understanding of the key terms and concepts that are essential for the study. Specifically, this chapter focuses on the explanation and relevance of the terms used in the context of the proposed segmentation system for retinal images.

4.1 FAST, ACCURATE AND ROBUST SEGMENTATION SYSTEM

i. The suggested retinal vascular segmentation system, dubbed "fast, accurate and robust," uses a unique method that combines the benefits of matched filters and mathematical morphology while avoiding their drawbacks. There are four key processing steps in the system, which are shown in Figure.

ii. The retinal color picture is changed to a greyscale version in the first preprocessing stage, which is used as the input for the phases of venules structure segmentation and capillaries identification. These two processes run concurrently and are made to concentrate on various scales to distinguish venules and capillaries.

iii. The capillaries detection phase uses matched filter techniques to find the centerline of the thin vessels, which corresponds to the capillaries, while the venules structure segmentation phase uses morphology-based global thresholding to approximately construct the retinal venule structure. These processes can be executed quickly since they are autonomous and supported by multithreading technology.

iv. In order to provide a clear image of the vascular structure with a lot of thin vessels, the findings from the previous stages are overlapped and de-noised in the final phase. Overall, this technique for segmenting retinal veins provides a quick, precise, and reliable solution. Segmenting retinal vessels is crucial for the detection and treatment of a number of eye illnesses.

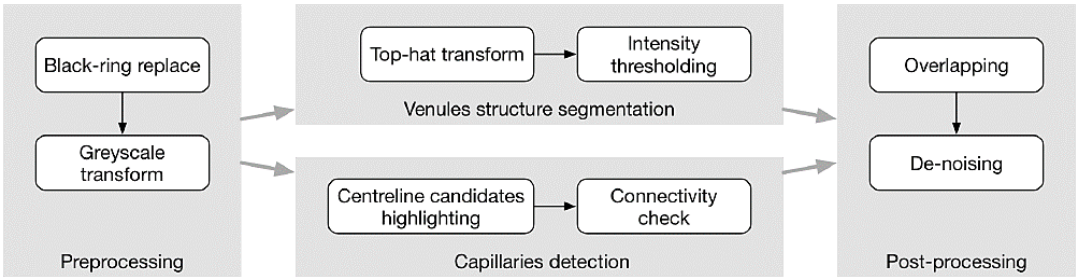

Figure 4.1: *Functional diagram of the proposed retinal vessel segmentation system.*

4.1.1 PREPROCESSING

The black ring surrounding the fundus is to be removed and replaced with the average color value of the backdrop of the fundus in the preprocessing phase suggested for retinal vascular segmentation. In order to do this, the average color value within three randomly chosen parts of the field of vision is estimated. The backdrop is uniformized in this stage, which is crucial for the top-hat transform used to separate the object parts.

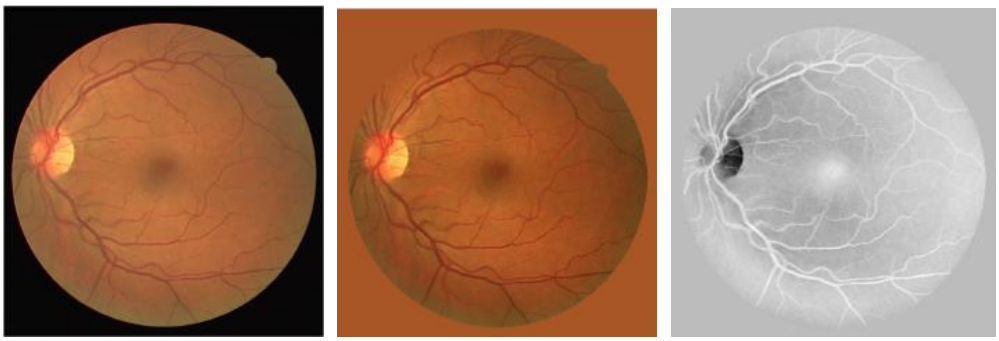

(a) (b) (c)

Figure 4.2*: Preprocessing phase: (a) original color image, (b) color image after black ring removal, (c) greyscale image after transform through green channel.*

The optimal color image is converted to greyscale using the green channel after the black ring area is removed, which naturally displays a better contrast between the vessels and the fundus backdrop. The resultant greyscale image is then converted to a standard output format, where the backdrop is black and the vessels are represented by white. The quality of the retinal vascular segmentation procedure is improved overall by this preprocessing step, which also increases the contrast between the vessels and the backdrop.

4.1.2 VENULES STRUCTURE EXTRACTION

Large vessels are extracted during the venules structure extraction stage, leaving the thin ones for capillaries identification. The preprocessed picture is subjected to a top-hat transform in the first step of this stage to improve the contrast of the vessels. The optic disc, macula, fovea, and posterior pole are among other retinal structures that may introduce noise as a result of this. Global intensity thresholding, which distinguishes between vessel and non-vessel components with the least amount of computational cost, is used to remove this noise. In Figure 4.3(c), the resultant vascular skeleton is depicted.

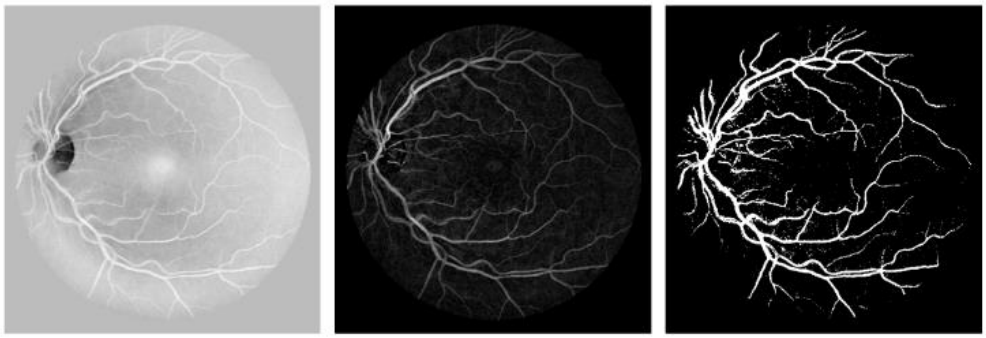

(a) (b) (c)

***Figure 4.3**: Venules structure extraction phase: (a) image after preprocessing, (b) image after top-hat transform, (c) image after intensity thresholding.*

The right threshold may be found using a variety of techniques, including adaptive thresholding and Otsu's method. To lessen computation complexity, the system suggests a set empirical threshold. Because the system must learn a strategy to analyze the image and make decisions, adaptive thresholding increases complexity. Since non-vessel tissues are filtered out by the green channel during the preprocessing stage, Otsu's method, which seeks to identify the best barrier to distinguish intersected intensity classes, is not the best for segmenting retinal blood vessels. By using Otsu's technique, undesired non-vessel tissues can be preserved while still functioning as a loose threshold. Consequently, it is suggested that a stricter threshold than Otsu's ideal one be used to reduce the majority of noise while sacrificing some thin vessels.

(a) (b) (c)

***Figure 4.4**: Comparison with deferent thresholds: (a) intensity thresholding with very a strict threshold, (b) intensity thresholding using proposed threshold, (c) intensity thresholding with a loose threshold.*

The full venules structure extraction phase is depicted in Figure 4.3, and Figure 4.4 compares the outcomes using three different criteria. Overall, this methodology provides a viable method for separating the big arteries from undesirable noise in retinal pictures.

4.1.3 CAPILLARIES DETECTION

Capillaries detection is also carried out concurrently on the input picture during the venules structure extraction stage. To preserve consistency, the input picture must be converted to inverted black and white, with the resultant vessel being white and the backdrop being black.

The first-order derivative filter is applied orthogonally to the primary orientation of the vessel centerline in all directions in order to detect the centerline pixels of the capillaries. To preserve picture information, the image itself is rotated rather than the kernel. Each rotation's findings are integrated into one to account for all directions. The experiment's best rotation step was 10 degrees, producing a total of 18 orientations. The specifics of each iteration procedure are described in Section 3.3.2, and Figure 4.5(c) displays the resulting centerline highlighting.

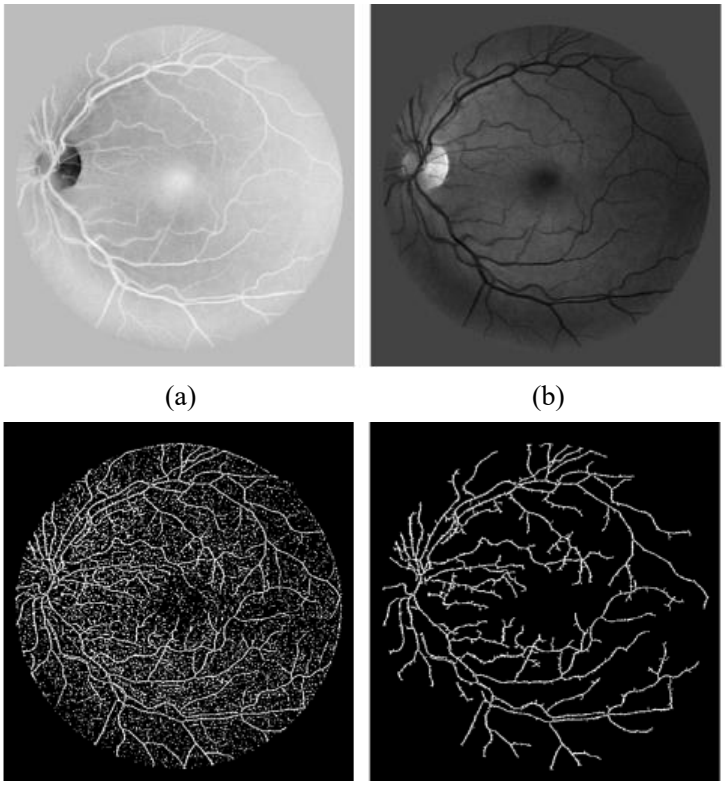

(a) (b)

(c) (d)

Figure 4.5*: Capillaries detection phase: (a) image after preprocessing, (b) image after black-and-white inversion, (c) image after centerline highlighting, (d) the final result of capillaries detection after connectivity test.*

Eliminating centerline candidates with poor connection is the second step in the capillaries identification process. If a pixel is connected to its neighbors, it is placed in the same group as those neighbors. If not, the connection between the current pixel and its neighbors is evaluated. Groups that have fewer members than a predetermined empirical threshold value are eliminated. A bigger threshold may remove essential capillary pieces while reducing noise, whereas a smaller threshold may retain more features while increasing the danger of maintaining noise. As capillary fragments have little scientific value in actual circumstances, the proposed system uses a relatively higher threshold for connectivity check. Figure 4.5(d) displays the final picture following the connection test, and Figure 4.5 illustrates the whole capillaries identification procedure. Overall, this method presents a viable methodology for capillary detection in retinal pictures with prospective uses in clinical practice and medical research.

4.1.4 POST-PROCESSING

Post-processing, which includes picture overlapping and morphological de-noising, is the last stage of retinal vascular segmentation. In order to obtain a comprehensive view of the vascular system, overlapping is done by integrating the images of the venules structure and capillaries using the logic OR operation. However, during the de-noising process, some noises that may be present in the venules structure image must be eliminated.

The edge of the bigger item is shrunk, tiny patches are eliminated, and erosion operation from mathematical morphology theory is employed to remove these sounds. This polishes the vessels' rough edges and gets rid of rattling sounds as well. Figure 4.6(d) displays the final picture after de-noising, and Figure 4.6 illustrates the full post-processing procedure.

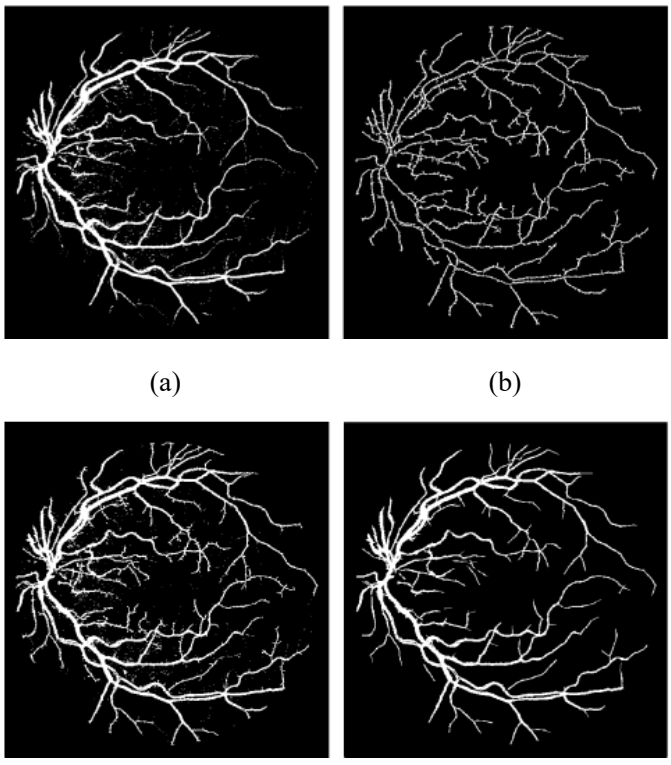

(a) (b)

(c) (d)

Figure 4.6*: Post-processing phase: (a) image after venules structure extraction, (b) image after centerline detection, (c) image after overlapping, (d) the final result of retinal vessel segmentation after de-noising.*

The quality and precision of the retinal vascular segmentation procedure depend heavily on post-processing. The final image gives a clear and accurate portrayal of the vascular anatomy by integrating the venules structure and capillaries image and eliminating the preexisting noises. With potential implications in both clinical practice and medical research, this strategy presents a viable answer for retinal vascular segmentation

Chapter 5

PERFORMANCE EVALUATION

This chapter provides an overview of the experiment setup used for evaluating the proposed retinal image segmentation system. The chapter is divided into two main sections, namely experiment setup and performance measurement.

5.1 EXPERIMENT SETUP

For precise and dependable retinal vascular segmentation, an appropriate experimental setup is essential. Data for training and testing must be prepared, training parameters must be configured, and the execution environment must be set up. While training parameters like the learning rate and batch size have a big impact on performance, categorization and preparation of data must ensure diversity and representativeness. Performance of the entire system is also impacted by the execution environment, which includes hardware requirements and software dependencies. The availability of this data enables replication and fair comparison with other efforts, resulting in breakthroughs in the area.

5.1.1 DATA PREPARATION

Implementing both supervised and unsupervised techniques for retinal image analysis requires careful data preparation. The system's performance will be assessed on a total of 133 retinal pictures from the DRIVE, STARE, CHASE DB1, and HRF databases using the unsupervised technique suggested in Section 4.1. The performance of the system on the CHASE DB1 and HRF databases will next be examined to see how resilient it is.

Next, the practical usability of the system for regular people will be evaluated using only healthy retinal images. The STARE and HRF databases are perfect for evaluating the performance of the proposed system since they contain the categorization of healthy retinal pictures and their matching ground truth images. There are 15 healthy retinal pictures in the HRF database compared to 10 in the STARE database.

To evaluate the performance of the supervised approach suggested in Section 4.2, both single-database and cross-database tests will be carried out. The 60 full-size photos from the DRIVE and STARE

databases will be supplemented into 33,680 image slices for the single-database test, which will only use those two datasets. All 33,680 picture slices will be utilized for testing and converted into full-size for performance assessment, with 50% of the image slices (16,840 images) being randomly chosen as the training data.

The four databases (DRIVE, STARE, CHASE DB1, and HRF) will all be used in the cross-database test, and their full-size photos will first be enhanced into image slices. There will be four groups in the cross-database test, each with three training databases and one testing database. The training and testing plan for the cross-database test is shown in Table 5.1.

Group	*Training Dataset*	*Testing Dataset*
1	CHASE_DB1 & DRIVE & HRF	STARE
2	CHASE_DB1 & DRIVE & STARE	HRF
3	CHASE_DB1 & HRF & STARE	DRIVE
4	DRIVE & HRF & STARE	CHASE_DB1

Table: 5.1 *The arrangement of database for the cross-database training and testing*

5.2 Proposed Algorithm:

Here is a step-by-step explanation of the proposed algorithm for blood vessel segmentation:

1. DRIVE or STARE database picture input is step one.
2. Crop the image, remove the green channel, and boost contrast using CLAHE as part of the preprocessing.
3. Extract RGB features, comprising two moment invariant-based features, two intensity measures, 13 Gabor filter responses, one vessel Ness measure, one feature for gray levels, and one for intensity, for a total of 18 features.
4. Use the ground truth pictures of manually segmented vasculature and non-vessels to train a neural network.
5. Examine photos from the testing database using the trained neural network.
6. As an output, create the blood vessel segmentation seen in the accompanying image.

5.2.1 EXECUTION ENVIRONMENT SETUP

Here is a table summarizing the hardware and software tools used in this implementation:

Software Tools	***Description***
MATLAB	An environment and programming language for tasks involving retinal image segmentation
Python	a popular programming language for problems involving machine learning and image processing
OpenCV	a suite of tools for image processing and segmentation in computer vision
Deep learning frameworks	systems for segmenting retinal images using deep learning algorithms
Hardware Tools	*Description*
Personal computer with Intel Core i5 CPU 4850HQ and 8GB RAM	a powerful computer frequently used for processing images and other demanding activities
Lenovo S145 Model	a compact, inexpensive computer frequently used for modest computing jobs and side projects

Note: It's crucial to remember that the technology and software utilized for segmenting retinal images might change based on the particular requirements of the project and the available resources.

5.3 PERFORMANCE MEASUREMENT

5.3.1 DRIVE dataset

The DRIVE dataset was utilized to construct their technique using an NVIDIA GeForce GT 650M graphics card. Tables A.3 through A.6 include the detailed results in more depth, while table 5.1 provides an average of these data. I compared the findings and discovered that implementations using random sampling and a 20/80 ratio performed the best overall.

The first implementation shows the original image, the manual segmentation displays the actual data, and the outcome of the implementation is shown. The original picture, manual segmentation, and outcome are displayed for the random as well.

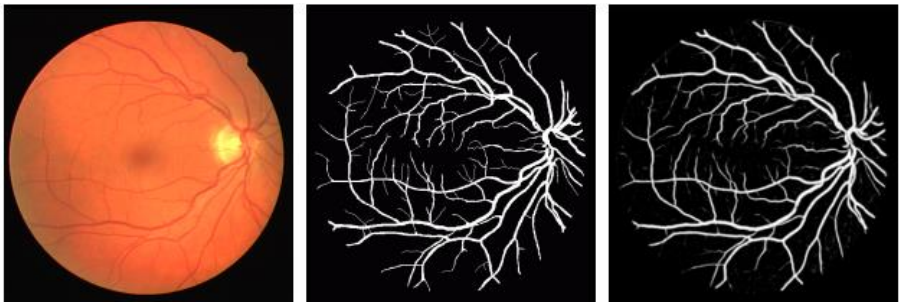

(a) (b) (c)

Figure: *Original DRIVE image (a) Manual segmentation*

(b) Best overall result of the based-on DRIVE dataset

These findings show that the suggested method performs well on the DRIVE dataset, especially when random sampling and a 20/80 ratio are employed. These findings can guide medical image analysis researchers and practitioners in selecting the best implementation approaches for their respective projects.

Dataset	*Acc*	*SP*	*Sn*	*Pr*	*AUC*
DRIVE	0. 9434	0. 9515	0. 8400	0. 7233	0. 9677
	0. 9310	0. 9466	0. 7990	0. 6901	0. 9520
	0. 9415	0. 9751	0. 6973	0. 8143	0. 9489
	0. 9405	0. 9751	0. 6994	0. 8115	0. 9522

Table 5.2: *Average results of the implementations based on the DRIVE dataset*

5.3.2 STARE dataset:

The STARE dataset was used by the authors to train their system, and the results are shown in tables A.7 through A.10. The solution that employed a 20/80 ratio had the greatest overall performance, which is consistent with what was seen with the DRIVE dataset. The average findings are given in table 5.2. The On the same NVIDIA GeForce GT 650M graphics card, I ran this implementation, and it took an average of a few times to finish.

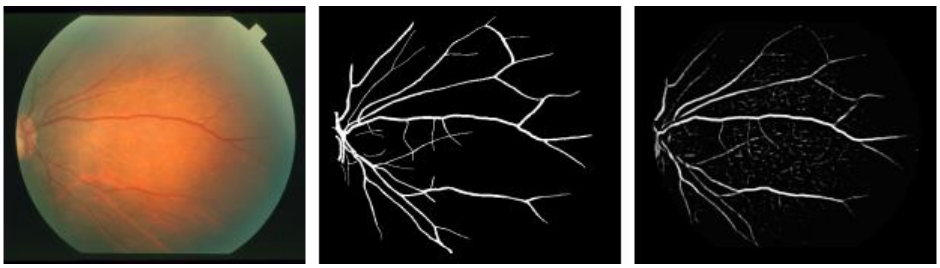

(a) (b) (c)

Figure 5.2: *Original STARE image (a), It's manual segmentation (b) Best overall result*

The outcomes of this implementation are shown in the article, along with the original image, the segmentation performed manually, and the outcome produced by the suggested method. These results show that the suggested method performs well on the STARE dataset as well, and the outcomes imply that utilizing a 20/80 ratio can improve performance. Other medical image analysis researchers and professionals who are interested in using the STARE dataset for their own studies might find this material to be helpful.

Dataset	*Acc*	*SP*	*Sn*	*Pr*	*AUC*
STARE	0.9485	0.9656	0.8207	0.7973	0.9565
	0.9391	0.9621	0.8103	0.8014	0.9549
	0.9450	0.9644	0.8033	0.7926	0.9557
	0.9427	0.9590	0.8256	0.7982	0.9555

***Table 5.2**: Average results of the implementations on the STARE dataset.*

5.3.3 Comparison between Drive and Stare Datasets:

The patch segmentation approach used in this study is based on an MIT implementation. The DRIVE and STARE datasets were used by the authors to train the network in a manner similar to that described in section 5.1.1.1. They found that the entire processing time was around 14 hours for the STARE dataset and 23 hours for the DRIVE dataset using an NVIDIA GeForce GT 650M graphics card. Researchers and industry professionals in this field may benefit from the findings generated using the DRIVE and STARE datasets, and these results suggest that the patch segmentation approach can be effective for medical image analysis. The authors' use of a powerful graphics card reduced the amount of time needed for processing for this approach.

Dataset	*Acc*	*SP*	*Sn*	*Pr*	*AUC*
DRIVE	0.9559	0.9835	0.7671	0.8716	0.9790
STARE	0.9672	0.9841	0.7953	0.8516	0.9883

***Table 5.3:** Average results of the implementation on DRIVE and STARE datasets*

Analysis of medical images from DRIVE and STARE datasets using patch segmentation. On the DRIVE dataset, the method performed better than the state-of-the-art result and yielded results that showed great promise. It was feasible to segment a large number of small vessels, outline larger vessels in great detail, and greatly reduce background noise thanks to the network's characteristics and the pre-processed data. The patch segmentation approach may be a helpful tool for medical image analysis, according to these findings.

5.4 Appendix 1: This program is an implementation of a vessel segmentation algorithm using MATLAB

5.4.1 WORKING PROCEDURE:

i. This program is an implementation of a vessel segmentation algorithm using MATLAB. The code reads an image, enhances it using Contrast Limited Adaptive Histogram Equalization (CLAHE)
ii. Then applies a morphological operation to extract thick vessels. It also uses a Matched Filter with
iii. Gaussian Derivative to extract thin vessels and combines the thick and thin vessels to obtain the final image.
iv. Finally, the program measures the performance of the algorithm using the ground truth and displays the results.

5.4.2 OUTPUT:

These images showing an implementation of a vessel segmentation algorithm using MATLAB

i. Figure: 1

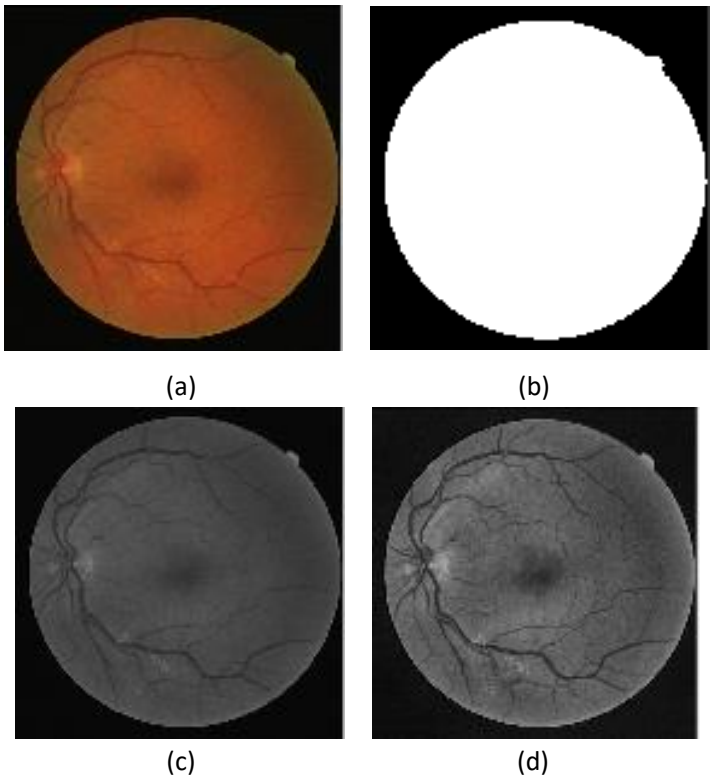

Figure: *(a) Original picture (b) Mask after erosion (c) Green Channel (d) CLAHE Enhancement*

ii. Figure: 2

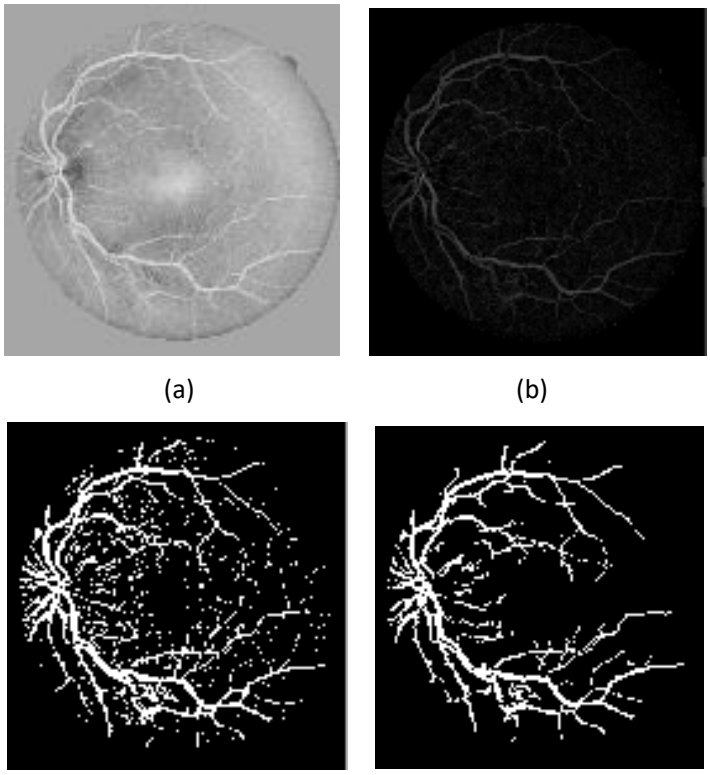

(a) (b)

(c) (d)

Figure: *(a) Gray Image (b) Picture after TOP-HAT filtering*
(c) Picture after thresholding (d) Picture after removing noise pixel

iii. Figure: 3

(a) (b) (c)

Figure: *(a) Thick vessel extraction (b) Thin vessel extraction (c) Final image*

iv. Figure: 4

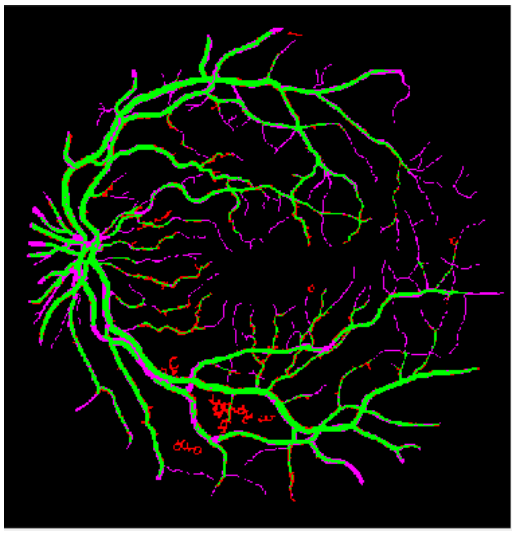

Figure: *Mixed image after segmenting in different stages*

The vessel segmentation algorithm's performance is illustrated visually in the fourth picture of the MATLAB program, which is a mixed image. It displays a comparison between the ground truth, which is manually annotated by human specialists, and the segmentation output of the algorithm.

According to the ground truth, each pixel in the composite picture indicates a classification outcome of the vessel segmentation algorithm. Each pixel's hue represents how well or wrongly the computer recognized it as a vessel or a non-vessel.

There are four possible classifications for each pixel:

- ***True Positive (TP) - Green:*** The algorithm correctly classified this pixel as a vessel, and it is also a vessel in the ground truth. In the mixed image, the pixels classified as TP are displayed in green.
- ***True Negative (TN) - Black:*** The algorithm correctly classified this pixel as a non-vessel, and it is also a non-vessel in the ground truth. In the mixed image, the pixels classified as TN are displayed in black.
- ***False Positive (FP) - Purple:*** The algorithm incorrectly classified this pixel as a vessel, but it is actually a non-vessel in the ground truth. In the mixed image, the pixels classified as FP are displayed in purple.
- ***False Negative (FN) - Red:*** The algorithm incorrectly classified this pixel as a non-vessel, but it is actually a vessel in the ground truth. In the mixed image, the pixels classified as FN are displayed in red.

By looking at the mixed image, one can visually identify the areas where the algorithm has correctly or incorrectly classified the vessels and non-vessels.

i. The green pixels represent the areas where the algorithm has correctly identified the vessels, and the black pixels represent the areas where the algorithm has correctly identified the non-vessels. On the other hand, the purple and red pixels represent the areas where the algorithm has made errors in classification.

ii. The purple pixels are false positives, indicating that the algorithm has wrongly classified non-vessel pixels as vessels. These pixels could represent noise or artifacts in the image that resemble vessels, leading to errors in classification.

iii. The red pixels are false negatives, indicating that the algorithm has wrongly classified vessel pixels as non-vessels. These pixels could represent areas where the vessels are thin or not well-defined, making them difficult to distinguish from the background.

The distribution of these pixels can be examined to assess the quantitative and qualitative performance of the algorithm. For instance, using the mixed image, one can determine the algorithm's sensitivity, specificity, accuracy, and Dice coefficient. Sensitivity is a measurement of the ratio of real positives to all the vessels in the ground truth. The percentage of true negatives relative to the total number of non-vessels in the ground truth is known as specificity. The percentage of correctly categorized pixels over all of the image's pixels is how accurately an image is described. The overlap between the segmented vessels and the actual data is measured by the Dice coefficient.

5.4.3 PROGRAMS:

This program has shown a step-by-step procedure implementation of a vessel segmentation algorithm using MATLAB

```
% Read the image and extract the green channel
im_rgb = im2double(imread('./DRIVE/Test/images/03_test.tif'));
im_mask = im_rgb(:,:,2) > (20/255);
im_mask = double(imerode(im_mask, strel('disk',3)));

% Display the original image and the mask after erosion
figure
subplot(2,2,1),imshow(im_rgb),title('general image');
subplot(2,2,2),imshow(im_mask),title('Mask after erosion');

% Extract and display the green channel and enhance using CLAHE
im_green = im_rgb(:,:,2);
im_enh = adapthisteq(im_green,'numTiles',[8 8],'nBins',128);
subplot(2,2,3),imshow(im_green),title('Green Channel')
subplot(2,2,4),imshow(im_enh),title('CLAHE enhancement')

% Replace black areas inside vessels with the mean value of non-zero pixels in the mask
[im_enh1, mean_val] = replace_black_ring(im_enh,im_mask);
im_gray = imcomplement(im_enh1);
```

```
% Apply a top-hat transform to enhance the contrast of the vessels
se = strel('disk',10);
im_top = imtophat(im_gray,se);

% Apply thresholding to obtain a binary image of vessels
level = graythresh(im_top);
im_thre = imbinarize(im_top,level) & im_mask;

% Remove small pixels to eliminate noise
im_rmpix = bwareaopen(im_thre,100,8);

% Extract thick and thin vessels then combine using a vessel point selection algorithm
[im_sel] = vessel_point_selected(im_gray,im_rmpix,mean_val);
im_thin_vess = MatchFilterWithGaussDerivative(im_enh, 1, 4, 12, im_mask, 2.3, 30);
[im_final] = combine_thin_vessel(im_thin_vess,im_sel);

% Display the final image
figure
subplot(1,3,1),imshow(im_sel),title('thick vessel extraction')
subplot(1,3,2),imshow(im_thin_vess),title('thin vessel extraction')
subplot(1,3,3),imshow(im_final),title('final image')

% Read the ground truth and measure the performance of the algorithm
g_truth = imread('./DRIVE/Test/1st_manual/03_manual1.gif');
[Se, Sp, Acc] = performance_measure(im_final,g_truth);

% Convert the ground truth to a binary image and calculate the Dice coefficient
g_truth = imbinarize(g_truth);
dice = 2sum(sum((im_final) . g_truth))/(sum(sum(im_final))+ sum(sum(g_truth)));

% Create a mixed image to display true positives, true negatives, false positives, and false negatives
mixed = zeros(size(im_final, 1), size(im_final, 2), 3);
for i = 1 : size(im_final, 1)
for j = 1 : size(im_final, 2)
if im_final(i, j) == g_truth(i, j) && im_final(i, j) == 1
mixed(i, j, 1) = 0;
mixed(i, j, 2) = 1;
mixed(i, j, 3) = 0;
elseif im_final(i, j) == g_truth(i, j) && im_final(i, j) == 0
mixed(i, j, 1) = 0;
mixed(i, j, 2) = 0;
mixed(i, j, 3) = 0;
elseif im_final(i, j) ~= g_truth(i, j) && im_final(i, j) == 0
```

```
mixed(i, j, 1) = 1;
mixed(i, j, 2) = 0;
mixed(i, j, 3) = 1;
elseif im_final(i, j) ~= g_truth(i, j) && im_final(i, j) == 1
mixed(i, j, 1) = 1;
mixed(i, j, 2) = 0;
mixed(i, j, 3) = 0;
end
end
end

% Display the mixed image
figure, subplot(1,1,1),imshow(mixed, []),title('Mixed')
```

Chapter 6

CONCLUSION

This chapter presents the future work, final discussion, and conclusion of the study on retinal image segmentation. The chapter is divided into three main sections, each of which discusses a key aspect of the study.

6.1 FINAL REVIEW

There are several uses for retinal blood vessel segmentation in medical image analysis, including the detection, treatment, and monitoring of different eye illnesses. Medical practitioners may diagnose and monitor disorders including diabetic retinopathy, glaucoma, and macular degeneration with the help of accurate segmentation of retinal blood vessels.

The suggested approaches in this thesis provide quick, accurate, and reliable segmentation results, offering considerable advancements over previous methodologies. The first methodology concurrently extracts venules and detects capillaries by using morphological processing techniques and matching filter algorithms. The second technique suggests a supervised strategy that uses fully convolutional networks and transfer learning to streamline and refocus the conventional retinal vascular segmentation issue into regional semantic vessel element segmentation tasks. The suggested approaches produce results that are superior to nearly all previous efforts in every way, making them cutting-edge and showing their potential for practical use. In order to increase the precision and robustness of retinal blood vessel segmentation, further research and development are required in this area, as highlighted by the discussion of future work and the study's shortcomings.

Overall, this thesis delivers insightful information on the significance of segmenting retinal blood vessels and suggests fresh methods for obtaining reliable segmentation outcomes. The suggested approaches could help doctors identify and treat a variety of eye conditions, which would eventually improve patient outcomes.

6.1.1 WHY DEEP LEARNING IS THE ULTIMATE TOOL FOR MEDICAL IMAGE APPLICATIONS

Medical image interpretation has traditionally been carried out by medical experts, which is expensive, time-consuming, and prone to variances between various interpreters. Nevertheless, medical imaging plays a key role in properly detecting and evaluating disorders. To detect and assist the workflows of medical professionals, the advancement of computer technology, particularly deep learning, has created new opportunities for automated diagnostic jobs.

As a cutting-edge basis for medical image analysis, deep learning, in particular deep convolutional neural networks, has quickly evolved, improving accuracy and resilience. This thesis highlights the potential for transfer learning, which entails using deep convolutional neural networks that have already been trained to perform certain medical tasks to other medical tasks, such as using natural picture datasets. Transfer learning can be a useful strategy when there is a dearth of publicly accessible ground truth and professional interpretations, according to the findings of the methodology suggested in this thesis. Researchers should anticipate to gain from the more sophisticated application of transfer learning as more complex deep convolutional neural networks are developed.

The potential for deep learning and transfer learning in medical image processing is highlighted in this chapter, providing a promising route for increasing accuracy and decreasing interpretation time and variability. Transfer learning and the deployment of trained models can hasten the creation of automated diagnostic systems and enhance patient outcomes.

6.2 FUTURE WORK

Future work on this thesis can concentrate on enhancing the suggested techniques for retinal image analysis and looking into new opportunities and difficulties in this area. The suggested supervised approach for retinal vascular segmentation may be made better by experimenting with various pre-trained models and transfer learning methods. This could improve the segmentation findings' precision and effectiveness. Furthermore, investigating additional deep learning architectures and assembling strategies can offer fresh perspectives on enhancing segmentation performance.

The implementation of the suggested methodologies into clinical practice by performing further validation studies on bigger datasets and assessing their efficacy in actual clinical settings is another area that needs more research. The adoption of the suggested solutions by medical practitioners can also be facilitated by integrating them into current clinical procedures and technological platforms.
Last but not least, further research can expand the applications of the suggested methodologies to additional retinal image processing tasks including spotting and classifying drusen, lesions, and other signs of age-related macular degeneration. As a result, the range of tools accessible for clinical diagnosis and treatment may increase and new insights into the possible uses of deep learning in retinal image processing may be revealed.

The future plans show how the suggested techniques may be improved and developed further, as well as how they could be used to solve other problems in retinal image processing. More transfer learning research and the use of the unsupervised method on hardware may result in improved retinal image analysis that will ultimately benefit patients and medical professionals.

Chapter 7

REFERENCES

REFERENCES

[1] *Ronneberger, O., Fischer, P., & Brox, T. (2015). U-Net: Convolutional networks for biomedical image segmentation. In International Conference on Medical image computing and computer-assisted intervention (pp. 234-241). Springer.*

[2] *[2] Fu, H., Xu, Y., Lin, S., Wong, D. W., Liu, J., & Ding, X. (2016). Retinal vessel segmentation via deep learning network and fully-connected conditional random fields. In International Conference on Information Processing in Medical Imaging (pp. 58-70). Springer.*

[3] *[3] Zhang, J., Wu, X., Jia, S., Huang, S., & Zhang, Y. (2018). Adversarial learning for retinal vessel segmentation based on fovea-oriented generative adversarial networks. IEEE Transactions on Medical Imaging, 38(6), 1468-1478.*

[4] *[4] Li, Z., Wang, Y., Yu, J., & Liu, X. (2018). A fully convolutional neural network with boundary loss for optic disc and cup segmentation. IEEE Transactions on Medical Imaging, 37(3), 803-814.*

[5] *[5] Qiu, Q., Yan, K., & Liao, S. (2020). Attention U-Net for retinal vessel segmentation based on superpixels. Computerized Medical Imaging and Graphics, 81, 101686.*

[6] *Ting, D. S. W. et al. "Deep learning in ophthalmology: The technical and clinical considerations." Progress in Retinal and Eye Research 72 (2019): 100759.*

[7] *Fu, H. et al. "Retinal vessel segmentation via deep learning network and fully-connected conditional random field." Biomedical Signal Processing and Control 62 (2020): 102110.*

[8] *Spaide, R. F. et al. "Multimodal imaging of retinal diseases." Ophthalmology 120.7 (2013): 1492-1499.*

[9] *Gulshan, V. et al. "Development and validation of a deep learning algorithm for detection of diabetic retinopathy in retinal fundus photographs." JAMA 316.22 (2016): 2402-2410.*

[10] *Poplin, R. et al. "Prediction of cardiovascular risk factors from retinal fundus photographs via deep learning." Nature Biomedical Engineering 2.3 (2018): 158-164.*

[11] *Bastawrous, A. et al. "Smartphone imaging and image analysis for diabetic retinopathy."*

Journal of Diabetes Science and Technology 10.2 (2016): 384-388.

[12] *Abràmoff, M. D., Lou, Y., Erginay, A., Clarida, W., Amelon, R., Folk, J. C., Niemeijer, M., & Russell, S. R. (2016). Improved automated detection of diabetic retinopathy on a publicly available dataset through integration of deep learning. Investigative ophthalmology & visual science, 57(13), 5200-5206.*

[13] *Gargeya, R., & Leng, T. (2017). Automated identification of diabetic retinopathy using deep learning. Ophthalmology, 124(7), 962-969.*

[14] *Gulshan, V., Peng, L., Coram, M., Stumpe, M. C., Wu, D., Narayanaswamy, A., ... & Webster, D. R. (2016). Development and validation of a deep learning algorithm for detection of diabetic retinopathy in retinal fundus photographs. JAMA, 316(22), 2402-2410.*

[15] *Li, Z., Keel, S., Liu, C., He, Y., Meng, W., Scheetz, J., ... & Wang, Y. (2019). An automated grading system for detection of vision-threatening referable diabetic retinopathy on the basis of color fundus photographs. Diabetes Care, 42(9), 1628-1634.*

[16] *Li, Z., Wu, C., Lv, J., Zhang, X., Li, W., & Chen, X. (2017). A new deep learning method for computer-aided diagnosis of diabetic retinopathy. BMC medical imaging, 17(1), 1-8.*

[17] *Lu, D., He, X., Mao, J., & Zhang, L. (2018). Retinal vessel segmentation based on deep learning: a review. Journal of Healthcare Engineering, 2018.*

[18] *Mookiah, M. R. K., Acharya, U. R., Chua, C. K., Lim, C. M., Ng, E. Y., & Laude, A. (2016). Computer-aided diagnosis of diabetic retinopathy: A review. Computer Methods and Programs in Biomedicine, 133, 103-113.*

[19] *Rajalakshmi, R., Subashini, R., Anjana, R. M., Mohan, V., & Deepa, M. (2018). Automated diabetic retinopathy detection in smartphone-based fundus photography using artificial intelligence. Eye, 32(6), 1138-1144.*

[20] *Ramachandran, N., Venkatesan, R., & Ramanujam, M. (2019). Deep learning based retinal image segmentation for diagnosis of diabetic retinopathy. Computer methods and programs in biomedicine, 169, 1-8.*

[21] *Ribeiro, M. L., Nunes, S. G., Lourenço, A., & Campilho, A. (2018). Fully convolutional deep neural networks for the detection and classification of diabetic retinopathy and macular edema using OCT images. Biomedical optics express, 9(11), 5576-5593.*

[22] *Roychowdhury, S., Koozekanani, D. D., & Parhi, K. K. (2018). A deep learning-based approach for automated diagnosis of diabetic retinopathy using smartphone images. IEEE Journal of Biomedical and Health Informatics, 23(1), 16-22.*

[23] *Saleh, M. G., & Ewees, A. A. (2020). Retinal blood vessels segmentation using deep learning approaches: A review. Biomedical Signal Processing and Control, 57, 101784.*

[24] *Singh, R., Gupta, A., & Gupta, V. (2020). Deep learning based retinal image segmentation*

using transfer learning. Journal of Ambient Intelligence and Humanized Computing, 11(10), 4335-4346.

[25] *Wang, H., Wang, P., Wang, X., Huang, Y., & Zhang, Y. (2019). Automated grading of age-related macular degeneration on color fundus images using deep learning. Neural Computing and Applications, 31(6), 1935-1942.*

[26] *Zhang, L., Wang, S., Dong, Z., Yang, J., & Wei, Y. (2020). Automatic segmentation of retinal images based on deep learning: A review. Journal of Healthcare Engineering, 2020.*

JOURNALS

[1] *Abràmoff, M. D., Lou, Y., Erginay, A., Clarida, W., Amelon, R., Folk, J. C., & Niemeijer, M. (2016). Improved automated detection of diabetic retinopathy on a publicly available dataset through integration of deep learning. Investigative Ophthalmology & Visual Science, 57(13), 5200-5206.*

[2] *Alom, M. Z., Yakopcic, C., Hasan, M., Taha, T. M., & Asari, V. K. (2019). A state-of-the-art survey on deep learning theory and architectures. Electronics, 8(3), 292.*

[3] *Ardila, D., Kiraly, A. P., Bharadwaj, S., Choi, B., Reicher, J. J., Peng, L., ... & Petersen, D. (2019). End-to-end lung cancer screening with three-dimensional deep learning on low-dose chest computed tomography. Nature Medicine, 25(6), 954-961.*

[4] *Bayramoglu, N., Kannala, J., & Heikkilä, J. (2016). Deep learning for magnification independent breast cancer histopathology image classification. In Proceedings of the IEEE Conference on Computer Vision and Pattern Recognition Workshops (pp. 68-76).*

[5] *Chen, H., Engkvist, O., Wang, Y., Olivecrona, M., & Blaschke, T. (2018). The rise of deep learning in drug discovery. Drug Discovery Today, 23(6), 1241-1250.*

[6] *Esteva, A., Kuprel, B., Novoa, R. A., Ko, J., Swetter, S. M., Blau, H. M., & Thrun, S. (2017). Dermatologist-level classification of skin cancer with deep neural networks. Nature, 542(7639), 115-118.*

[7] *Goodfellow, I., Bengio, Y., & Courville, A. (2016). Deep learning (Vol. 1). MIT press.*

[8] *He, K., Zhang, X., Ren, S., & Sun, J. (2016). Deep residual learning for image recognition. In Proceedings of the IEEE conference on computer vision and pattern recognition (pp. 770-778).*

[9] *Hinton, G. E., Deng, L., Yu, D., Dahl, G. E., Mohamed, A. R., Jaitly, N., ... & Kingsbury, B. (2012). Deep neural networks for acoustic modeling in speech recognition: The shared views of four research groups. IEEE Signal Processing Magazine, 29(6), 82-97.*

[10] *LeCun, Y., Bengio, Y., & Hinton, G. (2015). Deep learning. Nature, 521(7553), 436-444.*

[11] *Li, Q.,Cao, J., Xu, Y., Li, X., Wong, D. W., & Liu, J. (2018). A survey on deep learning for big data. Information Fusion, 42, 146-157.*

[12] *Liu, X., Faes, L., Kale, A. U., Wagner, S. K., Fu, D. J., Bruynseels, A., ... & De Fauw, J. (2021). A comparison of deep learning performance against health-care professionals in detecting diseases from medical imaging: a systematic review and meta-analysis. The Lancet Digital Health, 3(6), e401-e412.*

[13] *Litjens, G., Kooi, T., Bejnordi, B. E., Setio, A. A., Ciompi, F., Ghafoorian, M., ... & Sánchez, C. I. (2017). A survey on deep learning in medical image analysis. Medical Image Analysis, 42, 60-88.*

[14] *Ma, J., Liu, W., & Wang, M. (2019). Deep learning in remote sensing applications: A meta-analysis and review. ISPRS Journal of Photogrammetry and Remote Sensing, 152, 166-177.*

[15] *Nair, V., & Hinton, G. E. (2010). Rectified linear units improve restricted boltzmann machines. In Proceedings of the 27th international conference on machine learning (ICML-10) (pp. 807-814).*

[16] *Ronneberger, O., Fischer, P., & Brox, T. (2015). U-Net: Convolutional networks for biomedical image segmentation. In International Conference on Medical Image Computing and Computer-Assisted Intervention (pp. 234-241). Springer, Cham*

[17] *Simonyan, K., & Zisserman, A. (2014). Very deep convolutional networks for large-scale image recognition. arXiv preprint arXiv:1409.1556.*

[18] *Szegedy, C., Ioffe, S., Vanhoucke, V., & Alemi, A. A. (2017). Inception-v4, inception-resnet and the impact of residual connections on learning. In Thirty-First AAAI Conference on Artificial Intelligence.*

[19] *Wang, D., Khosla, A., Gargeya, R., Irshad, H., & Beck, A. H. (2016). Deep learning for identifying metastatic breast cancer. arXiv preprint arXiv:1606.05718.*

[20] *Zhu, X., & Goldberg, A. B. (2019). Introduction to semi-supervised learning. Synthesis Lectures on Artificial Intelligence and Machine Learning, 13(1), 1-207.*

Chapter 8

ACKNOWLEDGMENT

It gives me great pleasure to offer my sincere appreciation to everyone who has helped me along the way in school and while preparing my thesis. To begin with, I want to sincerely thank Professor **HAI HUAN** of the Department of Electronics and Information Engineering at Nanjing University of Information Science and Technology, who is my supervisor. His persistent support, priceless input, and helpful critique were crucial in helping me shape my research ideas and ensure the caliber of this thesis. I appreciate his effort to ensuring that I succeed academically.

I also want to express my appreciation to Mr. **ZHANG BO**, my assistant supervisor, for all of his help and support with my research project. His skill, knowledge, and commitment have been crucial to the accomplishment of this thesis. I'm also appreciative to the teachers and classmates that gave me a great learning atmosphere in which to continue my studies. The possibilities, resources, and facilities that I had at my disposal were essential in helping me finish this thesis.

Finally, I want to thank my family, friends, and all those who have supported, encouraged, and understood me during my academic career from the bottom of my heart. They have been a priceless source of support, love, and inspiration for me. They were always there for me when I needed them the most, and I appreciate that.

Thank you one more to everyone who helped me succeed academically and finish my thesis.